Polytetrafluoroethylene thin films obtained by the pulsed electron beam deposition method at different gas pressures

Roman Jędrzejewski[1)], Joanna Piwowarczyk[1), *)], Konrad Kwiatkowski[1)], Jolanta Baranowska[1)]

DOI: dx.doi.org/10.14314/polimery.2017.743

Abstract: Polytetrafluoroethylene (PTFE) coatings were manufactured using the pulsed electron beam deposition (PED) technique. The presence of a PTFE structure was confirmed by means of Fourier transform infrared spectrometry (FT-IR). The surface morphology and roughness were characterized by atomic force microscopy (AFM). A pressure increase leads to a decrease in the material transport from the target to the substrate. The water contact angle (*WCA*) and surface free energy (*SFE*) were examined. The hydrophobic properties were preserved after film deposition.

Keywords: polytetrafluoroethylene thin film, pulsed electron beam deposition, background gas pressure, chemical structure, hydrophobicity, surface free energy.

Cienkie powłoki politetrafluoroetylenowe otrzymane metodą pulsacyjnej ablacji elektronowej w warunkach zmiennego ciśnienia

Streszczenie: Cienkie powłoki z politetrafluoroetylenu (PTFE) wytwarzano metodą pulsacyjnej ablacji elektronowej (PED) z zastosowaniem zmiennego ciśnienia gazu roboczego. Techniką spektroskopii w podczerwieni z transformacją Fouriera (FT-IR) potwierdzono strukturę chemiczną osadzonej cienkiej warstwy. Za pomocą mikroskopii sił atomowych (AFM) oceniano morfologię i chropowatość otrzymanej powierzchni. Wyznaczono kąt zwilżania (*WCA*) i swobodną energię powierzchniową (*SFE*) powłok z PTFE. Stwierdzono, że zachowują one hydrofobowe właściwości politetrafluoroetylenu. Zwiększenie wartości zastosowanego w procesie ciśnienia wpłynęło na zmniejszenie grubości osadzanej warstwy PTFE w wyniku pogorszenia transportu materiału z targetu (tarczy) do podłoża.

Słowa kluczowe: cienkie powłoki politetrafluoroetylenowe, pulsacyjna ablacja elektronowa, ciśnienie gazu roboczego, struktura chemiczna, hydrofobowość, swobodna energia powierzchniowa.

Polytetrafluoroethylene (PTFE) is a synthetic polymer that is often used as a coating because of its chemical and mechanical properties. Amongst the important mechanical properties of PTFE coatings are their flexibility at low temperatures, low coefficient of friction, and stability at high temperatures [1, 2]. Other properties of great importance include high chemical resistance to corrosive reagents, insolubility in the majority of organic solvents, long-term weatherability, nonflammability, and hydrophobicity [2, 3]. Consequently, PTFE can be used in many applications in branches such as: mechanics, microelectronics, chemistry, medicine, and bioscience [1, 4]. On the other hand, these properties, for example non-stick behavior, are problematic for the manufacturing of thin PTFE coatings by traditional methods like spin coating, drop coating, and spray coating due to the poor adhesion of PTFE coatings to their substrates. Coatings are often required to preserve the properties of the bulk material, thus, methods that cause no changes in the chemical and surface morphology are desirable.

Recent research has demonstrated that PTFE coatings can be successfully deposited by means of pulsed laser deposition (PLD). The majority of studies confirmed that the chemical composition of the materials remained the same after deposition [1, 5, 6].

Although the PLD technique is well known and useful for obtaining PTFE films, pulsed electron beam deposition (PED) can be a promising alternative to this end. This is an advanced technique and the newest in film coating manufacturing that enables the deposition of very thin films with a well-controlled stoichiometry [7]. So far, PTFE coatings deposited by the PED technique have not been extensively studied. As yet, only a few attempts have been made [2, 7, 8]. Chandra and co-workers [7, 8] only concentrated in their work on the crystallinity of PTFE films. Other properties of the coatings were not studied. Henda and co-workers [2] prepared PTFE films on glass and silicon substrates. The process condi-

[1)] West Pomeranian University of Technology, Institute of Materials Science and Engineering, Al. Piastów 19, 70-310 Szczecin, Poland.

[*)] Author for correspondence; e-mail: joanna.piwowarczyk@zut.edu.pl

tions (background gas – argon, nitrogen; gas pressure, substrate temperature, discharge voltage) were widely varied. However, despite the extensive work carried out by the authors it is difficult to directly correlate the film properties and the deposition parameters. This may be attributable to the fact that too many parameters were changed simultaneously.

In this paper, we extend the research on the deposition of PTFE thin films by the PED technique. The aim is to clarify the influence of changes in the gas pressure on film thickness, chemical structure and coating morphology. The present studies in particular focus on the preservation of the chemical structure and hydrophobic properties of the material after the deposition process. This is the first work that shows the results of both *SFE* (surface free energy) and *WCA* (water contact angle) measurements for PTFE coatings obtained by PED methods.

EXPERIMENTAL PART

Preparation of samples

In the experiments, PTFE coatings were deposited by means of a PED system (NEOCERA, Inc. USA). The setup consisted of a vacuum chamber and a PEBS-20 pulsed electron source. PTFE coatings were obtained on monocrystalline Si (100) substrates, 10 x 10 mm in size. The Si substrates were sonically cleaned in an acetone bath, rinsed in acetone and isopropyl alcohol and dried in an air flow. A 99 % purity PTFE bulk disk was used as a target for the PED deposition. The chamber was evacuated to 0.1 mPa using nitrogen as the background gas. The PTFE film deposition took place at pressures of 0.4, 0.67, 0.93 and 1.46 Pa at room temperature. The deposition time was the same for all coatings, corresponding to 5000 pulses. The distance between the target and substrate was set at 80 mm. The electron source was operated at 12 kV with a repetition rate of 5 Hz.

Methods of testing

– The film thickness was estimated by measuring the step between the coating and an uncoated part of the substrate that remained covered during deposition. For these measurements, a profilometer (Dektak 6M, Veeco) was used with a 1 mg force and 12.5 μm stylus radius.

– The chemical structures were characterized using attenuated total reflection Fourier transform infrared spectroscopy (ATR-FTIR; Lumos, Bruker). 64 scans at a resolution of 4 cm^{-1} were carried out for each sample. Each spectrum was collected with an air background and corrected for CO_2 and H_2O. All spectra are presented after baseline correction and in the wave number range 600–4000 cm^{-1}.

– The contact angle and surface free energy were determined by means of a goniometer (DSA 100, Kruss), using a de-ionized water drop of volume 3 μm for the contact angle measurements. Surface free energy was calculated according to the Owen-Wendt model [9] from the contact angle of de-ionized water and diiodomethane.

– The surface topography and roughness were examined using atomic force microscopy (AFM; Veeco NanoScope IVa); 5.0 x 5.0 μm images were obtained in contact mode. The global surface arithmetic average roughness (R_a), including surface droplets, was measured for a 5.0 x 5.0 μm area. In addition, the average R_a value was also determined for the area between the droplets on five 0.2 μm^2 areas.

RESULTS AND DISCUSSION

Thickness and topography

Measurements with the profilometer indicated that the thickness of the coatings decreases linearly from about 200 nm to above 100 nm as the deposition pressure increased (Fig. 1).

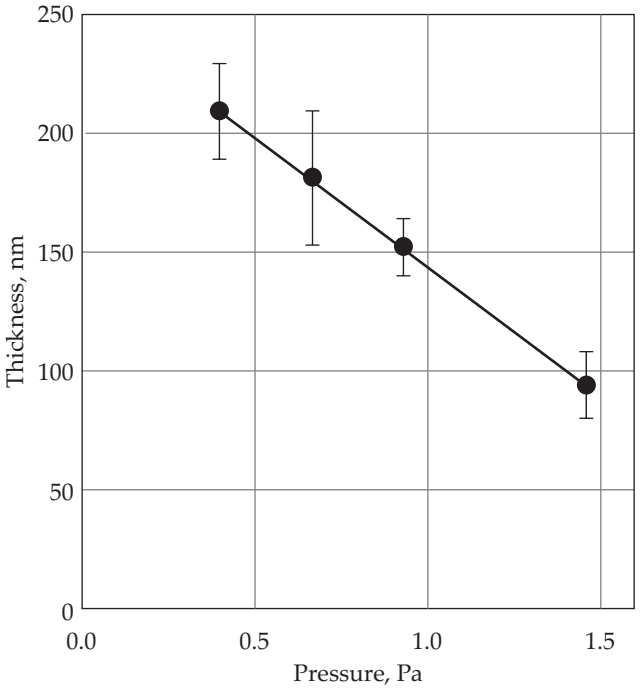

Fig. 1. Thickness of the coatings depending on the nitrogen pressure in the chamber

Figure 2 shows AFM, 5 x 5 μm, 3D images of the surface morphology of the films. The coatings deposited at 0.4, 0.67 and 0.93 Pa show a similar surface topography. A grain-like structure and a few small spikes were observed. The highest points on the film surface are probably droplets. The coating obtained at 1.46 Pa is different from the others: the number of spikes is greater and there are more uneven regions. This observation correlates well with the arithmetic average (R_a) roughness results presented in Fig. 3.

In this case, the R_a was obtained by measurements of an entire 5 x 5 μm surface. The roughness of the film deposited at 1.46 Pa is much higher than those depicted at

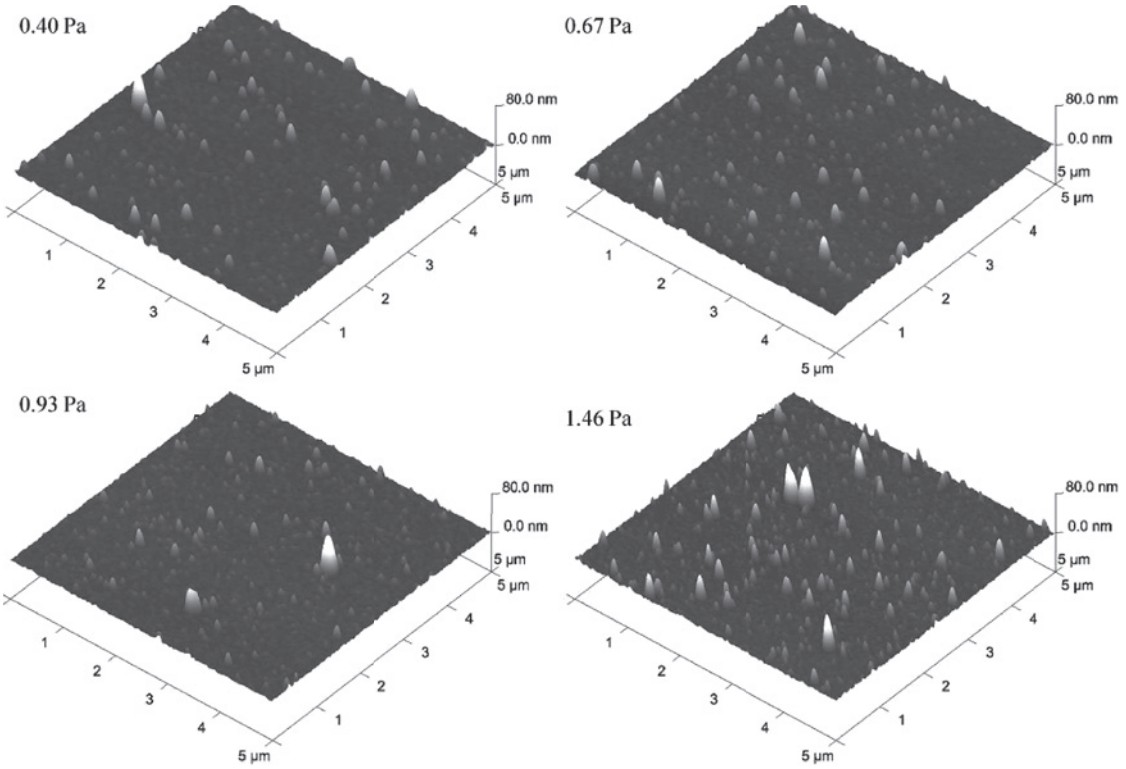

Fig. 2. Three-dimensional AFM images of the PTFE coatings obtained after deposition at different nitrogen pressures

the lower nitrogen pressures. Line 2 in Fig. 3 presents the relationship between the nitrogen pressure during the deposition process and the R_a obtained from five measurements of separated 0.2 µm^2 areas without droplets.

An increase in roughness with increasing pressure was also observed by other researchers. Stelmashuk and co-workers [10] observed a roughness dependence on the gas pressure for radio-frequency (rf) sputtering PTFE films. A roughness increase from below 1 to 40 nm was reported for a pressure range of 1–70 Pa. The roughness value of below 1 nm obtained at a pressure of 1 Pa correlates well with the values obtained in our experiments. The significant increase of roughness observed by them for the highest gas pressure was caused by droplet formation. An increase of droplet numbers with an increase of gas pressure was also observed in our experiments (Fig. 2) and by other researchers [2].

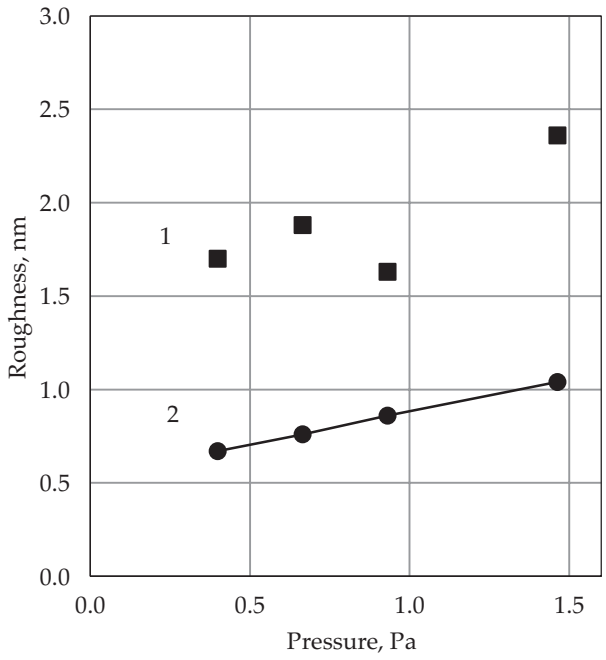

Fig. 3. R_a roughness of surface areas of PTFE coatings obtained at different deposition nitrogen pressures: droplets excluded, ■ droplets included

An increase of gas pressure reduces the mean free path of both electrons and polymer species ablated from the target. This first phenomenon leads to a decrease in the effective electron energy deposited in the target. Therefore, there is a growing tendency for melting the polymer target instead of ablating it and, as a consequence, a larger number of droplets are formed. The second phenomenon can reduce the kinetic energy of ablated material. In this way, the amount of species arriving at the substrate is lower and the coatings thinner as observed in our experiments. Moreover, due to the lower energy, the deposited molecules demonstrate a reduced mobility at the substrate surface, which could explain the observed increase in roughness between droplets.

Structure characterization

Figure 4 shows the FT-IR spectra of the PTFE target material that was used for deposition and of all obtained coatings and the Si substrate. It is worth mentioning that the Si substrate shows only one weak peak at approxi-

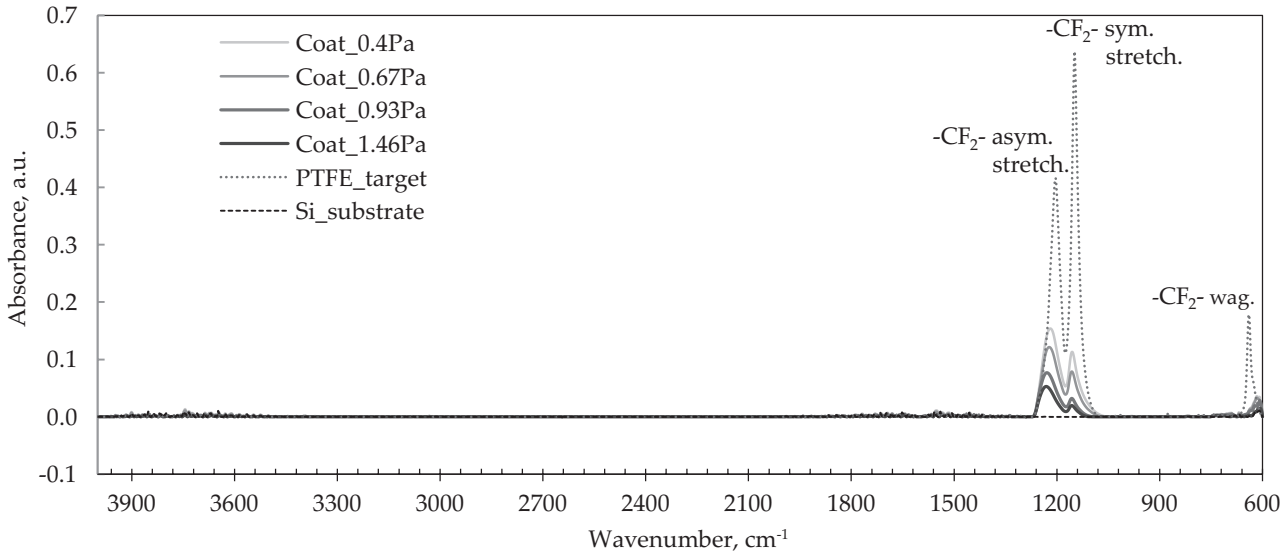

Fig. 4. FT-IR spectra of the PTFE coatings, target material and silicon substrate

mately 610 cm^{-1}. The two characteristic peaks at 1201 cm^{-1} and 1150 cm^{-1}, which can be seen in the spectrum of the PTFE target, are attributed to asymmetric and symmetric -CF_2- stretching vibrations. A third, weaker peak observed at 642 cm^{-1} corresponds to the -CF_2- wagging vibrations. These observations are consistent with literature data [2, 5, 7, 8]. All the PTFE coating spectra have characteristic -CF_2- stretching peaks at approximately 1220 cm^{-1} and 1154 cm^{-1}. Figure 5 shows the relationship between the coating thickness and the intensity of the symmetric and asymmetric -CF_2- stretching peaks. The intensity of these peaks increases with larger coating thickness, which is a result of the fact that the coating thickness is smaller than the material thickness analyzed by the FT-IR detector.

In the literature, evidence of chemical changes to the PTFE following the deposition process are reported as the presence of new peaks. For instance, peaks have been registered in the ranges: 1720–1730 cm^{-1}, corresponding to -FC=CF- stretching vibrations, as well as 730–740 cm^{-1} and 968–991 cm^{-1}, corresponding to -CF_3 deformation vibrations [10, 11]. In the present studies, no additional peaks were observed.

In summary, it can be stated that the FT-IR spectra analysis of the coatings does not indicate any major chemical differences compared to the target material. Notwithstanding, some differences can be observed between the spectra obtained for the PTFE coatings and that of the target material. The -CF_2- wagging peak of

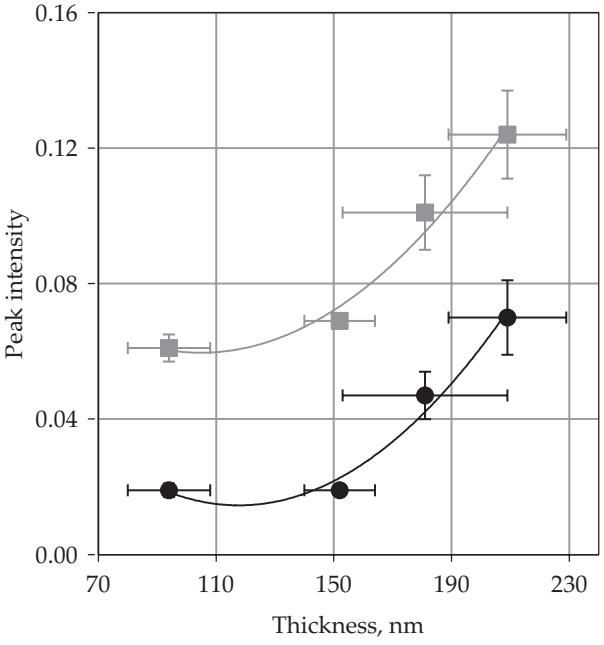

Fig. 5. Relationship between thickness of coatings and intensity of -CF_2- stretching peaks: ■ about 1220 cm^{-1}, ● about 1150 cm^{-1}

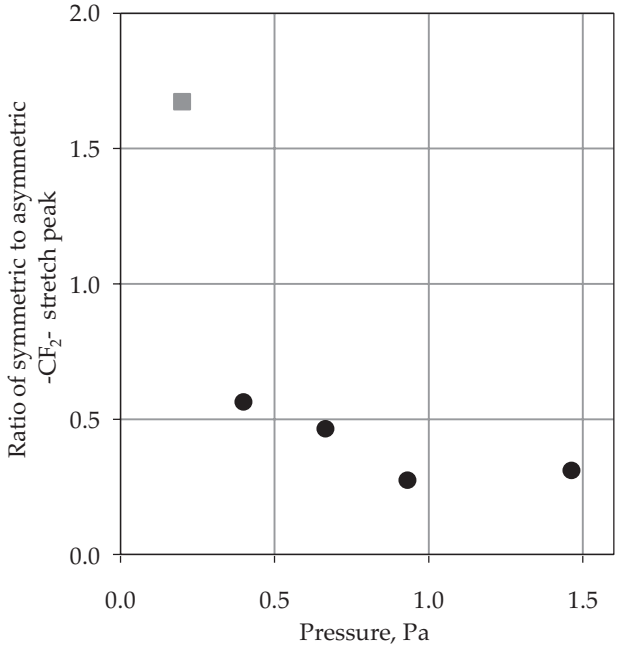

Fig. 6. The ratio of symmetric to asymmetric -CF_2- stretching peak intensity obtained from the different coatings by FT-IR spectra: ■ PTFE target, ● PTFE coatings

the coatings is shifted towards lower wave numbers in comparison to the position of the same peak registered for the target material. This can be due to the weak absorption nature of this peak [2] or the influence of the silicon substrate peak. Moreover, for all coatings, the asymmetric -CF_2- stretch peak has a greater intensity than the symmetric -CF_2- stretch peak, which is not the case for the PTFE target. Figure 6 presents the ratio of symmetric to asymmetric -CF_2- stretch peak intensities calculated from the spectra obtained for the different coatings and the target material. One of the reasons for the observed differences could be the small thickness of the layers, because in such a case the Si substrate peaks appear in the polymer spectrum and can disrupt its original shape. However, the results of Lauer and Bunting [12] did not show any changes in this peak ratio in the FT-IR spectrum obtained for a very thin, monomolecular PTFE film formed by rubbing a PTFE sheet against a smooth surface of stainless steel. Another reason for this phenomenon could be a reduction of the molecular mass of PTFE and polymer cross-linking due to deposition. Because the movements of the fluorine atoms are gradually reduced as the degree of cross-linking of the polymer increases, it could promote an increase in the number of the asymmetric stretching modes at the expense of symmetric ones. The confirmation of this hypothesis, however, requires further research.

Contact angle

Measurements of the water contact angle enable additional information to be obtained on the surface characteristics as it often correlates with changes in surface roughness [2, 5, 13] or chemical structure [10, 14].

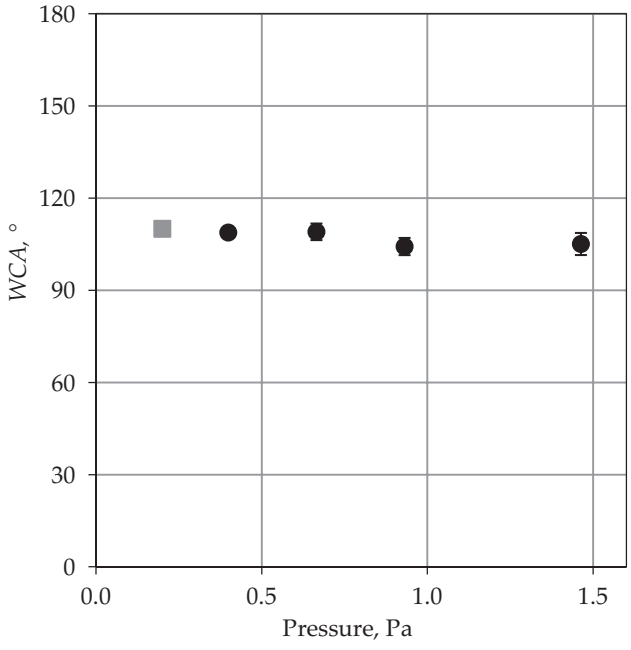

Fig. 7. The water contact angle (*WCA*) for PTFE target and coatings deposited at different pressures: ■ PTFE target, ● PTFE coatings

Figure 7 shows the relationship between the water contact angle and the deposition pressure. No major changes in water contact angle were observed. The obtained coatings have similar values as the target material of about 110°, which is also consistent with literature data [10, 15]. This shows that the hydrophobic character of the PTFE material remained unchanged after deposition. Henda *et al*. [2] reported a significant drop in the water contact angle after reaching a certain pressure level (*ca.* 0.26 Pa for argon and *ca.* 0.5 Pa for nitrogen) during the deposition of PTFE coatings by the PED method. They related these observations to surface morphology: a larger size of particulates and a lower surface density, which according to the Cassis and Baxter law could lead to the reduction of water contact angles. Such an explanation can be true for the materials with *WCA* below 90° as measured in their work. Our coating material demonstrates clear hydrophobic properties (Fig. 7) so the geometrical changes of surface topography would rather lead to an increase of *WCA*, which was not observed. Stelmashuk *et al*. [10] observed an increase of *WCA* with higher argon pressures for PTFE films deposited by rf sputtering. Changes in the chemical structure, mainly an increase in the number of -CF_3 groups, were considered to be the main cause of the increased hydrophobicity of the coatings. Atta *et al*. [14] demonstrated that the formation of polar groups occurs during plasma etching due to polymer interactions with oxygen atoms, which can increase the hydrophilic properties of the PTFE film. Takahashi *et al*. [15], however, have shown that different plasmas can induce the modification of the surface, leading to polymer main chains or C-F bonding scissions and thus increasing the hydrophobic properties of PTFE.

In our research, the observed changes in the coating roughness and morphology are rather small so it can be assumed that their influence on the water contact angle is not likely to be significant. On this basis, the observation that the *WCA* of both the deposited PTFE film and of the target material are the same can be considered as further evidence that the chemical structure of the PTFE material was not affected by the deposition process.

Surface free energy

The surface free energy of the films was calculated according to the Owen-Wendt model [9] using the contact angle of de-ionized water and diiodomethane.

The surface free energy (*SFE*) is the sum of the dispersion force and the polar force [16]:

$$\gamma_s = \gamma_s^d + \gamma_s^p \quad (1)$$

where: γ_s – the *SFE*, γ_s^d – the dispersive component, and γ_s^p – the polar component.

The *SFE* and its components for two measured liquids (water and diiodomethane) are shown in Table 1.

T a b l e 1. Surface free energy of two liquids used in the experiments [17]

Liquid	Surface free energy γ_s mJ/m^2	Polar component γ_s^p mJ/m^2	Dispersive component γ_s^d mJ/m^2
Water	72.8	51.0	21.8
Diiodomethane	50.8	0.0	50.8

The polar and dispersive components of the examined material were calculated from [9]:

$$(\gamma_s^d)^{0.5} = \frac{\gamma_d(\cos\theta_d + 1) - \sqrt{\left(\frac{\gamma_d^p}{\gamma_w^p}\right)}\gamma_w(\cos\theta_w + 1)}{2\left(\sqrt{\gamma_d^d} - \sqrt{\gamma_d^p\left(\frac{\gamma_w^d}{\gamma_w^p}\right)}\right)} \quad (2)$$

$$(\gamma_s^p)^{0.5} = \frac{\gamma_w(\cos\theta_w + 1) - 2\sqrt{\gamma_s^d\gamma_w^d}}{2\sqrt{\gamma_w^p}} \quad (3)$$

where: γ_s^d – the dispersive component of the *SFE* of the examined materials, γ_s^p – the polar component of the *SFE* of the examined materials, γ_d – the *SFE* of diiodomethane, γ_d^d – the dispersive component of the diiodomethane *SFE*, γ_d^p – the polar component of the diiodomethane *SFE*, γ_w – the *SFE* of water, γ_w^d – the dispersive component of the water *SFE*, γ_w^p – the polar component of the water *SFE*, θ_d – the contact angle of diiodomethane, and θ_w – the contact angle of water.

Figure 8 shows example snapshots of the PTFE target and film deposited at 0.67 Pa. The contact angle for water is approximately 110° (Fig. 8a, c) and the contact angle for diiodomethane is about 85° (Fig. 8b, d). The results of the investigation of the *SFE* for the PTFE coatings and the PTFE target are presented in Fig. 9.

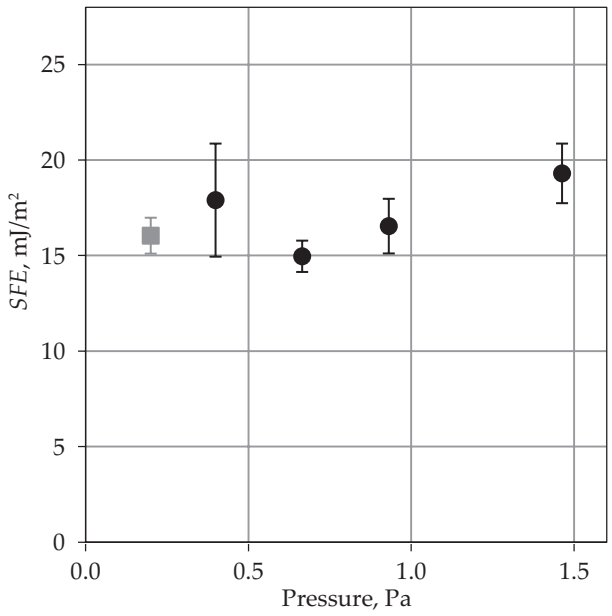

Fig. 9. The surface free energy (*SFE*) of the coatings deposited at different pressures: ■ PTFE target, ● PTFE coatings

The *SFE* values obtained are in the range of 14.9 mJ/m^2 to 19.3 mJ/m^2 for the PTFE coatings. This is comparable to the value of 16.04 mJ/m^2 obtained for bulk PTFE. In addition, the results are consistent with the results presented in the literature, where the *SFE* of bulk PTFE is reported to be in the range of 18.5 mJ/m^2 to 20.0 mJ/m^2 [18–20]. The most important result is that the obtained *SFE* values are low, and that the PTFE coatings retain a non-adhesive

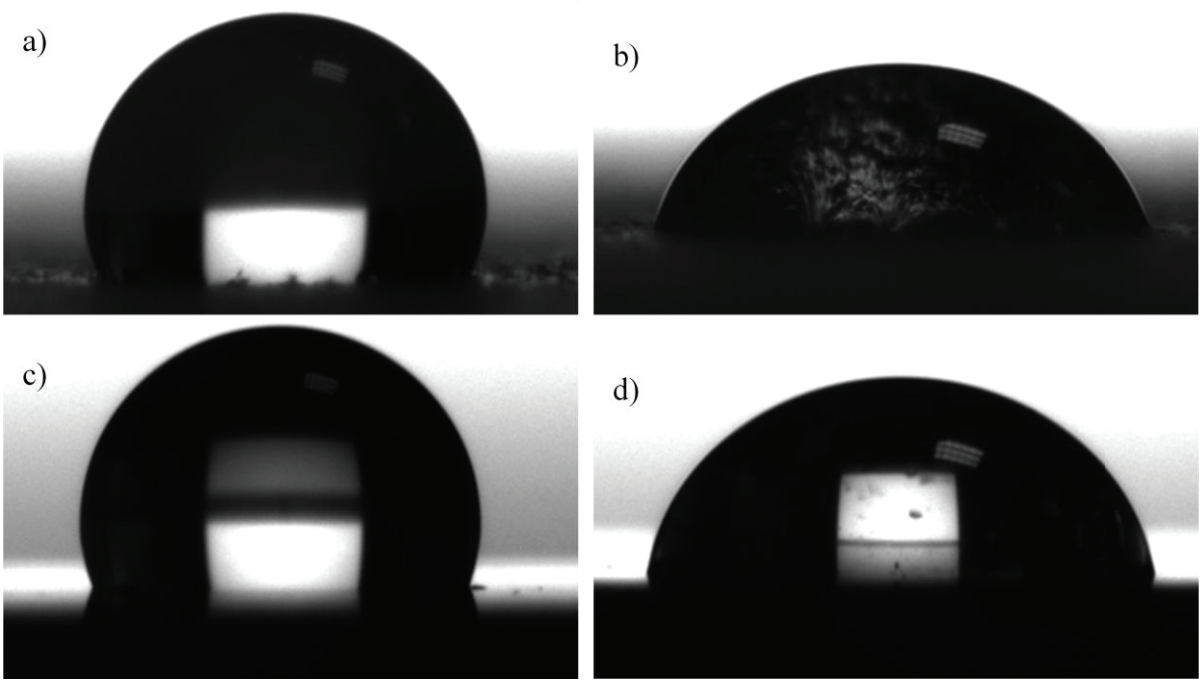

Fig. 8. Snapshots of: a) water drop on the PTFE target, b) CH_2I_2 on the PTFE target, c) water drop on the PTFE film deposited at 0.67 Pa, d) CH_2I_2 on the PTFE film deposited at 0.67 Pa

character. Moreover, the nearly constant *SFE* values are additional evidence of the presence of a stable chemical PTFE structure in the coatings.

CONCLUSIONS

The influence of gas pressure on the chemical structure and properties of PTFE thin films deposited by PED techniques were studied. The results are promising from the viewpoint of applying this technique for polymer film manufacturing. FT-IR analysis did not show any major changes in the chemical structure of the coatings deposited at any of the gas pressures used. Moreover, the hydrophobic properties of the PTFE were preserved after film deposition.

The gas pressure used in the deposition process has an important influence on the deposition rate and the coating morphology. The pressure increase leads to a decrease in material transport from the target to the substrate and to an increase in the number of droplets.

REFERENCES

[1] Li S.T., Arenholz E., Heitz J., Bauerle D.: *Applied Surface Science* **1998**, *125*, 17. http://dx.doi.org/10.1016/S0169-4332(97)00398-X

[2] Henda R., Wilson G.J., Gray-Munro J. *et al*.: *Thin Solid Films* **2012**, *520*, 1885. http://dx.doi.org/10.1016/j.tsf.2011.09.035

[3] Khan S.M., Franke R., Lehmann D., Heinrich G.: *Tribology International* **2009**, *42*, 890. http://dx.doi.org/10.1016/j.triboint.2008.12.014

[4] Schwödiauer R., Bauer-Gogonea S., Bauer S. *et al*.: *Applied Physics Letters* **1998**, *73*, 2941. http://dx.doi.org/10.1063/1.122637

[5] Kwong H.Y., Wong M.H., Wong Y.W., Wong K.H.: *Applied Surface Science* **2007**, *253*, 8841. http://dx.doi.org/10.1016/j.apsusc.2007.04.036

[6] Daoud W.A., Xin J.H., Zhang Y.H., Mak C.L.: *Thin Solid Films* **2006**, *515*, 835. http://dx.doi.org/10.1016/j.tsf.2005.12.245

[7] Chandra V., Manoharan S.S.: *Applied Surface Science* **2008**, *254*, 4063. http://dx.doi.org/10.1016/j.apsusc.2007.12.045

[8] Chandra V., Manoharan S.S.: *Metal-Organic and Nano--Metal Chemistry* **2008**, *38*, 288.

[9] Rudawska A., Jacniacka E.: *International Journal of Adhesion & Adhesives* **2009**, *29*, 451. http://dx.doi.org/10.1016/j.ijadhadh.2008.09.008

[10] Stelmashuk V., Biederman H., Slavínská D. *et al*.: *Vacuum* **2005**, *77*, 131. http://dx.doi.org/10.1016/j.vacuum.2004.08.011

[11] Katoh T., Zhang Y.: *Applied Surface Science* **1999**, *138–139*, 165. http://dx.doi.org/10.1016/S0169-4332(98)00395-X

[12] Lauer J.L., Bunting B.G., Jones W.R.: *NASA Technical Memorandum* **1987**, *89844*, 1.

[13] Miller J.D., Veeramasuneni S., Drelich J. *et al*.: *Polymer Engineering & Science* **1996**, *36*, 1849. http://dx.doi.org/10.1002/pen.10580

[14] Atta A., Fawzy Y.H.A., Bek A. *et al*.: *Nuclear Instruments and Methods in Physics Research Section B* **2013**, *300*, 46. http://dx.doi.org/10.1016/j.nimb.2013.02.004

[15] Takahashi T., Hirano Y., Takasawa Y. *et al*.: *Radiation Physics and Chemistry* **2011**, *80*, 253. http://dx.doi.org/10.1016/j.radphyschem.2010.07.042

[16] Fowkes F.M.: *Industrial and Engineering Chemistry* **1964**, *56*, 41. http://dx.doi.org/10.1021/ie50660a008

[17] Ström G., Fredriksson M., Stenius P.: *Journal of Colloid and Interface Science* **1987**, *119*, 352. http://dx.doi.org/10.1016/0021-9797(87)90280-3

[18] Oya T., Kusano E.: *Vacuum* **2008**, *83*, 564. http://dx.doi.org/10.1016/j.vacuum.2008.04.040

[19] Liu Z., Rogachev A.V., Zhou B. *et al*.: *Progress in Organic Coatings* **2011**, *72*, 321. http://dx.doi.org/10.1016/j.porgcoat.2011.05.003

[20] Farhatnia Y., Tan A., Motiwala A. *et al*.: *Biotechnology Advances* **2013**, *31*, 524. http://dx.doi.org/10.1016/j.biotechadv.2012.12.010

Received 2 I 2017.